Korean Journal of Radiology

KJR

Check for updates

T2 Mapping with and without Fat-Suppression to Predict Treatment Response to Intravenous Glucocorticoid Therapy for Thyroid-Associated Ophthalmopathy

Linhan Zhai[1, 2], Qiuxia Wang[1], Ping Liu[3], Ban Luo[4], Gang Yuan[5], Jing Zhang[1]

Departments of [1]Radiology, [4]Ophthalmology, and [5]Endocrinology, Tongji Hospital, Tongji Medical College, Huazhong University of Science and Technology, Wuhan, China; [2]Department of Radiology, Xiangyang Central Hospital, Affiliated Hospital of Hubei University of Arts and Science, Xiangyang, China; [3]Department of Medical Imaging, Guangdong Second Provincial General Hospital, Guangzhou, China

Objective: To evaluate the performance of baseline clinical characteristics and pretherapeutic histogram parameters derived from T2 mapping of the extraocular muscles (EOMs) in the prediction of treatment response to intravenous glucocorticoid (IVGC) therapy for active and moderate-to-severe thyroid-associated ophthalmopathy (TAO) and to investigate the effect of fat-suppression (FS) in T2 mapping in this prediction.

Materials and Methods: A total of 79 patients clinically diagnosed with active, moderate-to-severe TAO (47 female, 32 male; mean age ± standard deviation, 46.1 ± 10 years), including 43 patients with a total of 86 orbits in the responsive group and 36 patients with a total of 72 orbits in the unresponsive group, were enrolled. Baseline clinical characteristics and pretherapeutic histogram parameters derived from T2 mapping with FS (i.e., FS T2 mapping) or without FS (i.e., conventional T2 mapping) of EOMs were compared between the two groups. Independent predictors of treatment response to IVGC were identified using multivariable analysis. Receiver operating characteristic (ROC) curve analysis was performed to evaluate the predictive performance of the prediction models. Differences between the models were examined using the DeLong test.

Results: Compared to the unresponsive group, the responsive group had a shorter disease duration, lower kurtosis (FS-kurtosis), lower standard deviation, larger 75th, 90th, and 95th (FS-95th) T2 relaxation times in FS mapping and lower kurtosis in conventional T2 mapping. Multivariable analysis revealed that disease duration, FS-95th percentile, and FS-kurtosis were independent predictors of treatment response. The combined model, integrating all identified predictors, had an optimized area under the ROC curve of 0.797, 88.4% sensitivity, and 62.5% specificity, which were significantly superior to those of the imaging model (p = 0.013).

Conclusion: An integrated combination of disease duration, FS-95th percentile, and FS-kurtosis was a potential predictor of treatment response to IVGC in patients with active and moderate-to-severe TAO. FS T2 mapping was superior to conventional T2 mapping in terms of prediction.

Keywords: Thyroid-associated ophthalmopathy; Intravenous glucocorticoid therapy; Treatment response; Fat-suppression; T2 mapping; Magnetic resonance imaging

INTRODUCTION

Thyroid-associated ophthalmopathy (TAO), also known as Graves' ophthalmopathy, is a clinical manifestation of Graves' disease. Common symptoms of TAO are photophobia, excessive tearing, diplopia, eyelid retraction, exophthalmos, and swelling of periorbital tissues [1]. The recommended first-line treatment for active and moderate-to-severe TAO is high-dose intravenous glucocorticoid (IVGC) therapy; however, this treatment inevitably produces adverse effects

due to the toxicity of the administered glucocorticoids [2]. Approximately 20%–25% of patients with TAO do not respond effectively to IVGC therapy [3]. Therefore, identifying TAO patients who would truly benefit from IVGC before therapeutic administration is necessary to avoid ineffective treatment.

The acquisition of T2 mapping, entails a multi-spin-echo sequence and mono-exponential decay, and can be used to quantitatively analyze tissues by measuring T2 relaxation time (T2RT) [4,5]. This technique has become increasingly used in TAO in recent years for purposes such as staging [6], activity assessment [7], and evaluation of treatment response [8]. Extraocular muscles (EOMs) are the primary tissues involved in TAO and often present with enlarged fusiform configurations [9]. Pathological changes in active and moderate-to-severe TAO are primarily observed as inflammatory edema [10], but inflammation and fatty degeneration are usually synchronously present in EOMs in clinical practice. T2RT primarily reflects the water content of EOMs, and prolonged T2RT is closely associated with inflammatory edema in EOMs [11]. However, other contents such as fat can also increase T2RT and confound quantitative measurements [7]. Fat-suppression (FS) with chemical shift-selective saturation is a technique applied to remove the contribution of signal from fat in the signal from a tissue without interfering with the water signal [12]. We hypothesized that FS T2 mapping would perform better than conventional T2 mapping when evaluating inflammatory edema in EOMs.

Volumetric histogram analysis is a first-order statistical-based texture analysis that assesses tissue heterogeneity by analyzing the distribution of voxel gray levels in a given volume of interest (VOI) [13]. Previous studies [7,14] on T2 mapping were mostly based on the analysis of regions of interest (ROIs) and primarily focused on the mean T2RT, which is subjective and cannot fully utilize the capacity of T2 mapping. Volumetric histogram analysis of T2 mapping can provide more information about the VOI by analyzing the inhomogeneity of tissues. Therefore, the purpose of this study was to evaluate the performance of baseline clinical characteristics and pretherapeutic histogram parameters derived from T2 mapping of EOMs in predicting the treatment response to IVGC in patients with active and moderate-to-severe TAO and to investigate the effect of FS in T2 mapping on this prediction.

MATERIALS AND METHODS

Patients

This study was approved by our Institutional Review Board (IRB-ChiECRCT-20170087), and the requirement for written informed consent from the patients was waived because of the retrospective nature of the study. We enrolled 79 patients (47 female, 32 male; mean age ± standard deviation [SD], 46.1 ± 10.0 years) who were clinically diagnosed with active and moderate-to-severe TAO between April 2017 and December 2020 and treated in our eye clinic. The inclusion criteria were as follows: 1) patients who underwent orbital magnetic resonance imaging (MRI), based on the routine scanning protocol before treatment, 2) high-quality MRI guaranteed for further analysis, 3) patients who successfully completed standard IVGC administration, based on the consensus of the 2016 European Group on Graves' Orbitopathy Guidelines [2], 4) patients aged between 18 and 65 years, 5) disease duration of less than 18 months in patients with TAO, 6) both eyes of the patient exhibited TAO, 7) patients who did not have other orbital diseases, apart from TAO, and 8) IVGC alone without other therapies, such as radiotherapy and surgical decompression, used to manage patients with TAO.

Before IVGC therapy, an experienced ophthalmologist and endocrinologist evaluated the activity and severity of TAO based on procedures used in previous studies [15,16]. The clinical information of the patients was collected, which included sex, age, disease duration, clinical activity score (CAS), NOSPECS score, smoking habits, and hormone levels related to thyroid function. Based on the classification criteria used in previous studies [17,18], patients were classified into responsive and unresponsive groups, with responsiveness determined by their therapeutic response to IVGC within two weeks after the end of therapy.

Orbital MRI Scanning

Routine orbital MRI was conducted within 1 week before immunosuppressive therapy was initiated. A 3T MRI scanner (Discovery 750, GE) was used to complete the entire scanning process, which was placed with a 32-channel head coil. The patients were required to lay supine and keep their head fixed with a sponge to fit the head coil. During MRI scanning, the patients were instructed to close their eyes and keep their eyeballs immobile to reduce bothersome artifacts. The details of the scanning protocol are as follows:

Coronal T2 Iterative Decomposition of Water and Fat with Echo Asymmetric and Least-Squares Estimation (IDEAL)

Echo time (TE), 68 ms; repetition time (TR), 2200 ms; flip angle, 111°; matrix, 320 x 224; field of view (FOV), 20 cm; bandwidth, 63; number of excitations (NEX), 2; slice thickness, 3 mm; spacing, 0.6 mm; total slices, 15; scan time, 2 minutes 52 seconds.

Coronal FS T2 Mapping

Echo train length, 8; TE, 9.9–79.2 ms (ΔTE = 9.9 ms); TR, 2025 ms; matrix, 256 x 256; FOV, 20 cm; bandwidth, 21; NEX, 1; slice thickness, 3 mm; spacing, 0.6 mm; total slices, 15; and scan time, 8 minutes 43 seconds.

Coronal Conventional T2 Mapping

Echo train length, 8; TE, 9.9–79.2 ms (ΔTE = 9.9 ms); TR, 2000 ms; matrix, 256 x 256; FOV, 20 cm; bandwidth, 21; NEX, 1; slice thickness, 3 mm; spacing, 0.6 mm; total slices, 15; and scan time, 8 minutes 36 seconds.

Image Analysis

The T2 IDEAL images were first reviewed to evaluate inflammatory edema of the EOMs in patients with TAO (Fig. 1A, B). The original data of FS T2 mapping and conventional T2 mapping were post-processed using software (FireVoxel) in a Windows system. On the FS T2 mapping images, the medial, inferior, lateral, superior rectus, superior oblique, and inferior oblique muscles were manually drawn with ROIs, layer by layer, from the orbital apex to the posterior globe to cover the entirety of orbital EOMs, as much as possible. The superior rectus and levator palpebrae were considered as being a complex on imaging because of the difficulty in separating them. The ROIs were carefully delineated along the margin of the EOMs to avoid the effect of orbital fat, air in the maxillary sinus, and interposed fat between the superior rectus and levator palpebrae on some layers. When completing the delineation slice-by-slice, the total VOI of the six muscles of an orbit was obtained. The VOI was calculated using FireVoxel, and the following histogram parameters were acquired: T2RT values of minimum, maximum, mean, and SD, skewness, kurtosis, entropy, inhomogeneity, and cumulative parameters, which included the 5th, 10th, 25th, 50th, 75th, 90th, and 95th percentiles of T2RT values (Fig. 1C, D).

The imaging data from conventional T2 mapping were processed using the same method (Fig. 1E, F). Two experienced radiologists (observers 1 and 2, who had three and nine years of experience in neuroradiology, respectively), who were blinded to the study design and clinical information of patients, independently completed the quantitative measurements. Observer 1 remeasured the histogram parameters at 1-month intervals.

Statistical Analysis

The SPSS software (version 21; IBM Corp.) was used for all statistical analyses. An interclass correlation coefficient with a 95% confidence interval was used to assess the repeatability of the two measurements. Univariable logistic regression analysis was used to compare clinical characteristics between the responsive and unresponsive groups. Characteristics that met the requirements of $p < 0.05$ or an Odds ratio (OR) > 1.5 were included in the multivariable analysis. The histogram parameters were also compared between the two therapeutic response groups using univariable analysis. The normality of the parameters was examined using the Shapiro-Wilk test. Normally distributed data were analyzed using the unpaired t test, whereas non-normally distributed data were analyzed using the Mann-Whitney U test. The results are presented as the mean ± SD. All significant clinical variables and histogram parameters were simultaneously included in the multivariable analysis to determine the independent predictors of treatment response to IVGC. Receiver operating characteristic (ROC) curve analysis was conducted to evaluate the performance of the prediction models containing the identified predictors. Finally, the difference between the combined model, consisting of the identified clinical and imaging predictors, and the imaging model, including only the imaging predictors, was examined using the DeLong test. Statistical significance was set at $p < 0.05$.

RESULTS

Analysis of Patients' Clinical Characteristics

In total, 79 patients (158 orbits) (47 female, 32 male; mean age, 46.1 ± 10 years) with active and moderate-to-severe TAO met the inclusion criteria. The included patients were divided into a responsive group (n = 86 orbits) and an unresponsive group (n = 72 orbits) based on their therapeutic response. In the univariable logistic regression analysis, with the exception of disease duration ($p = 0.002$, OR = 0.901), no significant differences were found for sex (OR = 1.67), age (OR = 0.984), smoking habits (OR = 2.533), CAS (OR = 1.093), NOSPECS score (OR = 0.942), or serum
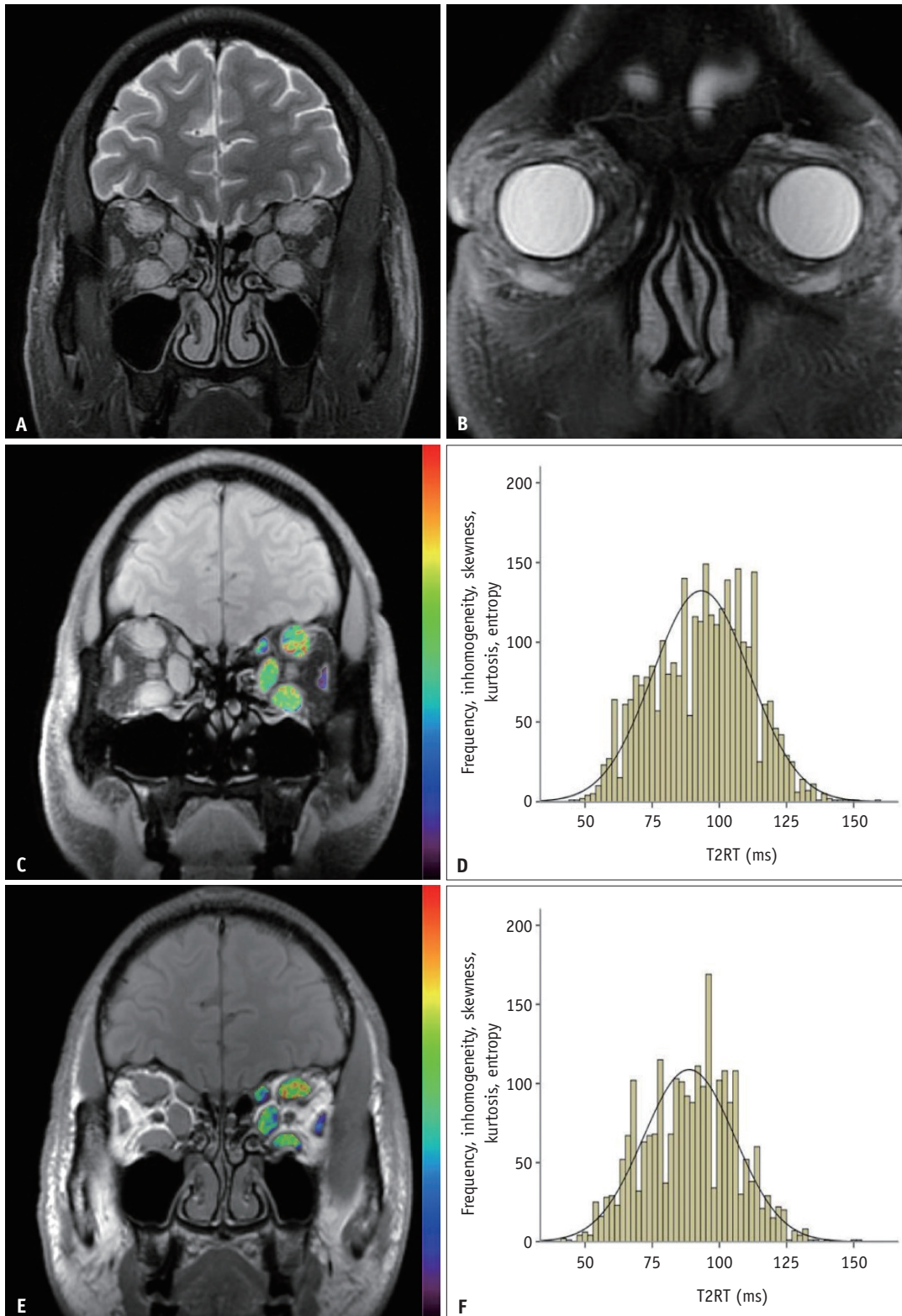
Fig. 1. A 60-year-old male with TAO.
A, B. Coronal T2 IDEAL imaging shows inflammatory edema of the medial, inferior, lateral, and superior rectus muscles, as well as the superior oblique and inferior oblique muscles. **C, D.** Coronal fat-suppression T2 mapping shows the VOI of the EOMs in the left orbit and the histogram derived from the VOI. **E, F.** Coronal conventional T2 mapping shows the VOI of the EOMs in the left orbit and the histogram derived from the VOI. EOM = extraocular muscle, IDEAL = iterative decomposition of water and fat with echo asymmetry and least-squares estimation, TAO = thyroid-associated ophthalmopathy, T2RT = T2 relaxation time, VOI = volume of interest

concentrations of T3 (OR = 1.24), T4 (OR = 1.094), thyroid-stimulating hormone (TSH) (OR = 0.99), and thyrotropin receptor antibody (OR = 0.998). Multivariable analysis, which included variables conforming to the criterion of $p < 0.05$, or OR > 1.5, revealed that disease duration ($p = 0.001$) was a significant clinical characteristic. The details of the analysis of the patients' clinical characteristics are shown in Table 1.

Analysis of Histogram Parameters

Intraobserver repeatability (0.990–0.993) and interobserver repeatability (0.982–0.987) were excellent for evaluating the repeatability of the measurements of histogram parameters derived from FS T2 mapping and conventional T2 mapping. Univariable analysis revealed that the responsive group compared with the unresponsive group had lower kurtosis ($p < 0.001$), lower SD ($p = 0.03$), and larger 75th, 90th, and 95th T2RTs ($p = 0.031$, $p = 0.028$, and $p = 0.026$, respectively) in FS T2 mapping and lower kurtosis in conventional T2 mapping ($p = 0.01$). A detailed analysis of the histogram parameters is presented in Table 2 and Figure 2.

Independent Predictors for Treatment Response to IVGC

Multivariable analysis, which included significant clinical variables and histogram parameters, showed that disease

Table 1. Univariable Analysis of Clinical Characteristics between Responsive Group and Unresponsive Group
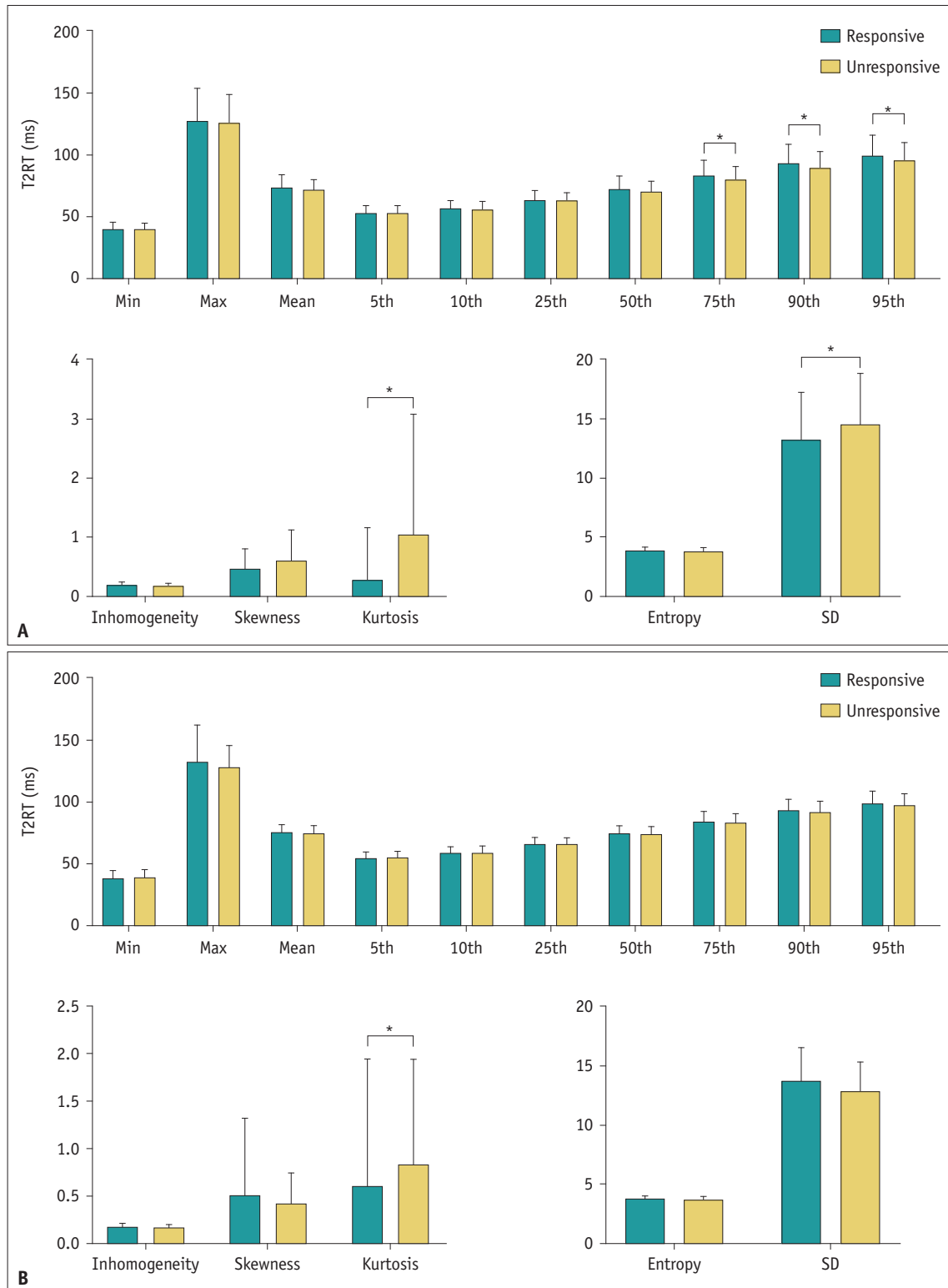
Parameters	Responsive (n = 43)	Unresponsive (n = 36)	Odds Ratio (95% CI)	P
Sex, female/male	28/15	19/17	1.670 (0.675–4.134)[†]	0.267
Age, year	45.4 ± 10.63	46.94 ± 9.34	0.984 (0.941–1.03)	0.493
Smoking, no/yes	38/5	27/9	2.533 (0.764–8.406)[†]	0.129
Disease duration, month	5.56 ± 4.32	8.42 ± 6.29	0.901 (0.844–0.962)	0.002*
CAS	3.37 ± 0.9	3.31 ± 0.86	1.093 (0.652–1.831)	0.735
NOSPECS score	6.21 ± 1.81	6.39 ± 1.69	0.942 (0.73–1.216)	0.648
Thyroid hormones				
TSH, uIU/mL	3.11 ± 6.5	3.64 ± 8.13	0.99 (0.931–1.053)	0.748
T3, pg/mL	4.02 ± 3.56	3.18 ± 1.02	1.24 (0.874–1.757)	0.228
T4, ng/L	14.67 ± 11.43	11.1 ± 3.67	1.094 (0.986–1.213)	0.091
Thyrotropin receptor antibody, IU/L	14.63 ± 12.85	15.02 ± 14.37	0.998 (0.965–1.031)	0.898

Data are mean ± standard deviation or number of patients, unless specified otherwise. Odds ratios were obtained using the odds of being in the responsive group as opposed to the unresponsive group; therefore, values > 1 indicate a positive association with the responsive group. *Indicates statistically significant results at $p < 0.05$, [†]Indicates results with Odds ratio > 1.5. CAS = clinical activity score, CI = confidence interval

Table 2. Univariable Analysis of Histogram Parameters between Responsive and Unresponsive Groups

Parameters	FS T2 Mapping			Conventional T2 Mapping		
	Responsive (n = 86)	Unresponsive (n = 72)	P	Responsive (n = 86)	Unresponsive (n = 72)	P
Min, ms	39.63 ± 5.99	39.68 ± 5.07	0.678	37.73 ± 6.68	38.53 ± 6.49	0.776
Max, ms	128.06 ± 25.71	125.74 ± 23.23	0.556	129.45 ± 20.8	127.4 ± 17.5	0.652
Mean, ms	73.9 ± 9.79	71.55 ± 8.61	0.093	74.91 ± 6.36	74.37 ± 6.1	0.726
SD	13.17 ± 4.02	14.53 ± 4.30	0.03*	13.6 ± 2.77	12.91 ± 2.39	0.128
Inhomogeneity	0.19 ± 0.05	0.18 ± 0.04	0.103	0.18 ± 0.03	0.17 ± 0.03	0.055
Skewness	0.47 ± 0.33	0.61 ± 0.51	0.077	0.40 ± 0.28	0.42 ± 0.32	0.526
Kurtosis	0.13 ± 0.51	1.05 ± 2.03	< 0.001*	0.60 ± 1.34	0.83 ± 1.11	0.01*
Entropy	3.84 ± 0.3	3.77 ± 0.30	0.142	3.81 ± 0.21	3.79 ± 0.19	0.651
5th, ms	52.95 ± 6.02	52.81 ± 5.67	0.756	54.47 ± 4.87	54.97 ± 4.87	0.515
10th, ms	56.51 ± 6.57	56.15 ± 5.98	0.673	58.52 ± 4.94	58.9 ± 5.02	0.634
25th, ms	63.26 ± 7.93	62.33 ± 6.83	0.397	65.45 ± 5.35	65.61 ± 5.19	0.842
50th, ms	72.42 ± 10.05	70.00 ± 8.56	0.09	73.97 ± 6.52	73.43 ± 6.09	0.817
75th, ms	83.36 ± 12.41	79.56 ± 11.06	0.031*	83.58 ± 8.05	82.43 ± 7.44	0.587
90th, ms	93.72 ± 14.71	89.21 ± 13.61	0.028*	92.72 ± 9.23	90.93 ± 9.09	0.303
95th, ms	100.48 ± 14.83	95.49 ± 14.73	0.026*	98.55 ± 9.80	96.71 ± 9.48	0.246

Data are mean ± SD. *Indicates statistically significant results at $p < 0.05$. FS = fat-suppression, SD = standard deviation

Fig. 2. Bar graphs show the comparison of histogram parameters, based on fat-suppression T2 mapping (A) and conventional T2 mapping (B), between the responsive group and the unresponsive group. *Indicates that the results are significantly different. SD = standard deviation, T2RT = T2 relaxation time

duration (p = 0.005), FS-95th percentile (p = 0.021), and FS-kurtosis (p = 0.002) were independent predictors of treatment response to IVGC therapy. The details of the multivariable analysis results are shown in Table 3.

ROC Curve Analysis

The imaging model, consisting of FS-95th and FS-kurtosis, yielded an area under the ROC curve of 0.714, sensitivity of 72.1%, and specificity of 55.6%. When integrating disease duration, FS-95th, and FS-kurtosis, the combined model yielded an ROC area of 0.797, a sensitivity of 88.4%, and a specificity of 62.5%. The DeLong test showed a statistically significant difference between the combined model and the imaging model (p = 0.013). The detailed results of the ROC curve analysis are presented in Table 4 and Figure 3.

DISCUSSION

In the present study, we compared the baseline clinical characteristics and pretherapeutic histogram parameters, based on FS T2 mapping and conventional T2 mapping, between treatment-responsive and treatment-unresponsive groups. Furthermore, we evaluated the performance of different prediction models in assessing the treatment response to IVGC therapy in patients with moderate-to-severe TAO. We found that FS T2 mapping was superior to

conventional T2 mapping in predicting treatment response to IVGC. The combined model, which included disease duration, FS-95th percentile, and FS-kurtosis, demonstrated significantly better predictive performance than imaging models that included FS-95th percentile and FS-kurtosis.

EOMs were visibly enlarged on MR images in most patients with TAO, but microscopic pathologic changes varied. Orbit fibroblasts are target cells of TAO and exhibit dysfunction through autoimmune mechanisms [19]. The phenotypic and functional heterogeneity of fibroblasts causes EOMs to occasionally develop coexisting inflammatory edema, fatty degeneration, and fibrosis in the same patient [20]. The SD represents the degree of dispersion from the mean values, and a lower SD indicates a more homogeneous T2RT distribution in the EOMs. Kurtosis reflects the peak properties of histogram based-T2 mapping [13]. Lower absolute kurtosis values indicated that fewer voxels of the EOMs deviated from the Gaussian distribution, which also indicated a more homogeneous T2RT distribution in the EOMs. Voxels of the EOMs were arranged based

Table 3. Multivariable Analysis of Predictors for Treatment Response to IVGC Therapy

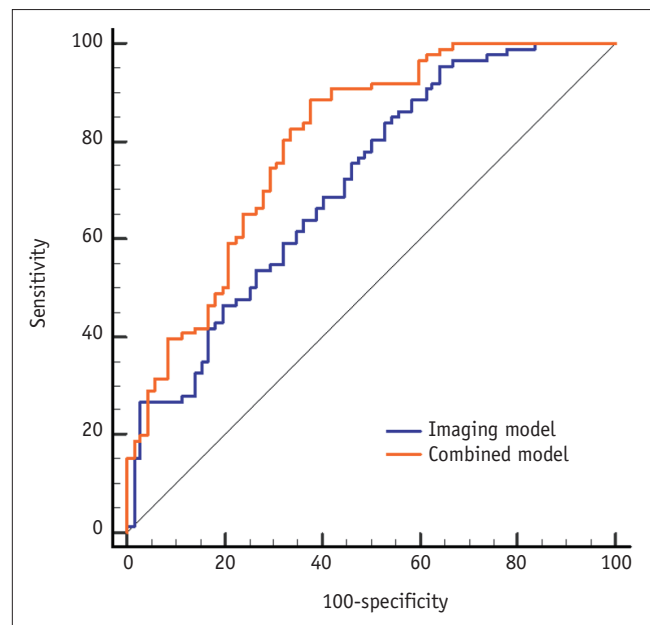| Parameters	OR (95% CI)	P
Disease duration, month	0.904 (0.843–0.970)	0.005*
Kurtosis	1.028 (0.724–1.460)	0.878
FS-standard deviation	0.933 (0.667–1.304)	0.683
FS-kurtosis	0.280 (0.125–0.627)	0.002*
FS-75th, ms	1.020 (0.823–1.262)	0.859
FS-90th, ms	0.736 (0.529–1.023)	0.068
FS-95th, ms	1.337 (1.046–1.710)	0.021*

ORs were obtained using the odds of being in the responsive group as opposed to the unresponsive group; therefore, values > 1 indicate a positive association with the responsive group. *Indicates statistically significant results at p < 0.05. CI = confidence interval, FS = fat-suppression, IVGC = intravenous glucocorticoid, OR = Odds ratio

Fig. 3. Receiver operating characteristic curve shows the predictive efficiency of the combined model and the imaging model.

Table 4. Predictive Efficiency of Single-Predictor Model and Multi-Predictor Model in Patients with TAO

Model	AUC (95% CI)	Sensitivity (%)*	Specificity (%)*
FS-95th + FS-kurtosis	0.714 (0.637–0.783)	72.1	55.6
Disease duration + FS-95th + FS-kurtosis	0.797 (0.726–0.857)	88.4	62.5

*The cutoff values for calculating sensitivity and specificity were those that gave the largest Youden index value (sensitivity + specificity - 1). AUC = area under the curve, CI = confidence interval, FS = fat-suppression, TAO = thyroid-associated ophthalmopathy

on the magnitude of the T2RT values in the histogram. Larger values in the high percentiles (i.e., 75th, 90th, and 95th percentiles) indicate that voxels with a high T2RT predominate in the EOMs. Increased T2RT values are closely associated with inflammatory edema in EOMs [21].

FS T2 mapping showed lower kurtosis and SD, with larger values in the high percentiles (75th, 90th, and 95th percentiles) in the responsive group than in the unresponsive group in the present study. This finding indicates that the responsive TAO group had more homogeneous edema, as reflected by the analysis of FS T2 mapping. However, both inflammatory edema and fatty degeneration increase T2RT values, the variance of which is difficult to distinguish [22,23]. Our results revealed that in conventional T2 mapping, the responsive group had lower kurtosis values without a corresponding larger value in the high percentile compared to the unresponsive group. This finding indicates that prolonged values in the high percentiles of T2RT in the unresponsive group may be caused by an increase in fat content. Therefore, the parameters of conventional T2 mapping cannot truly reflect inflammatory edema in EOMs. In addition, the results revealed that FS-95th percentile and FS-kurtosis were independent predictors, which further demonstrated that FS T2 mapping was superior to conventional T2 mapping in predicting treatment response to IVGC therapy.

We found that disease duration was an independent predictor, which coincided with the results of a previous study [8]. TAO consists of an active stage, characterized by hyaluronan synthesis, and an inactive stage, characterized by adipocyte proliferation and fibrosis [24,25]. The responsive group had a significantly shorter disease duration, indicating that the majority of responsive patients were in the early phase of the TAO process. This phase primarily includes interstitial edema, which is apt to have a good response to IVGC [26]. TAO occurs more commonly in women, whereas men present with more severe symptoms [27]. In our study, the responsive group comprised more female patients (OR = 1.67, $p > 0.05$), indicating that sex had no predictive value among the patients. The results showed that the unresponsive group comprised more patients who smoked (OR = 2.533, $p > 0.05$); however, smoking was not an independent predictor of treatment response. This finding is inconsistent with that of a previous study [28]. The limited sample size in our study cannot represent the entire population of TAO patients and may have resulted in this discrepancy.

Distinguishing responsive patients from unresponsive patients before they receive IVGC therapy is essential, as determining patients' likelihood of responsiveness minimizes the adverse effects related to unnecessary glucocorticoid administration and allows clinicians to administer other therapies (e.g., rituximab) in unresponsive patients at an earlier treatment stage, rather than after IVGC therapy has proved ineffective [29]. In the multivariable analysis, we found that the combined model, which included disease duration, FS-95th, and FS-kurtosis, showed significantly better predictive performance than the imaging model, which included FS-95th and FS-kurtosis (AUC = 0.797 and AUC = 0.714, respectively). Additionally, the sensitivity and specificity of the combined model (88.4% and 62.5%, respectively) were superior to those of the imaging model (72.1% and 55.6%, respectively). A previous study [30] integrated $T2RT_{95\%}$, skewness, and entropy to construct a nomogram to predict the treatment response of IVGC with a good accuracy of 0.792, which was similar to that of our combined model (0.797). In another study [31], $T2RT_{min}$ and disease duration were regarded as independent predictors and were incorporated to achieve the prediction, which had the highest specificity (100%) and the highest sensitivity (65%). In contrast, our combined model displayed unsatisfactory specificity (only 62.5%); however, the sensitivity was notable (88.4%). The present study indicates that clinicians should comprehensively consider clinical characteristics and imaging features to diagnose and evaluate TAO in clinical practice. Different examination methods reflect the disease characteristics from different perspectives. When integrating disease duration, FS-95th, and FS-kurtosis, the treatment response to IVGC can be effectively predicted before patients receive therapy, ensuring the implementation of personalized therapy.

Our study had several limitations. First, this retrospective study was conducted with a relatively small sample size, which was insufficient for performing further analyses (e.g., radiomics). Therefore, in-depth studies with a larger sample size are needed in the future for confirmation of our findings. Second, the collection of disease duration details from the patients may have been confounded by recall bias and differences in disease tolerance. Third, a prior medication history for hyperthyroidism was not collected as one of the clinical characteristics of this study. The control of hyperthyroidism is beneficial for the improvement of TAO in clinical practice. Consequently, the intrinsic relationships between these factors should be explored

in the future. Fourth, we could not analyze the whole volume of the EOMs because of the slice thickness and spacing in MRI scanning. Fifth, the entire scanning time was relatively long (approximately 20 minutes), inevitably resulting in eye movements in the subjects, particularly in older patients and those with severe TAO. Therefore, the scanning parameters and processes should be optimized in the future. Sixth, the manual segmentation of VOIs is inevitably erroneous, even though we took preventive measures (e.g., carefully drawing and repeatedly measuring) to ensure accuracy. Hence, semi-automated or automated segmentation is recommended in further studies.

In conclusion, the findings of this study indicate that combined baseline clinical characteristics and pretherapeutic histogram based-T2 mapping are valuable in predicting IVGC treatment response, and FS T2 mapping is superior to conventional T2 mapping for this purpose. The integration of disease duration and pretherapeutic FS-95th and FS-kurtosis values is a potential predictor of treatment response to IVGC therapy in patients with active and moderate-to-severe TAO. This combined model could be used to screen patients responsive to IVGC before starting IVGC therapy, which would allow clinicians to craft more individualized treatment strategies in clinical practice.

Availability of Data and Material

All data generated or analyzed during the study are included in this published article.

Conflicts of Interest

The authors have no potential conflicts of interest to disclose.

Author Contributions

Conceptualization: Linhan Zhai, Qiuxia Wang, Ping Liu, Jing Zhang. Data curation: Qiuxia Wang, Ban Luo, Gang Yuan. Formal analysis: Linhan Zhai, Ping Liu. Funding acquisition: Ping Liu, Jing Zhang. Investigation: Linhan Zhai, Qiuxia Wang, Ping Liu, Jing Zhang. Methodology: Linhan Zhai, Jing Zhang. Project administration: Jing Zhang. Resources: Qiuxia Wang, Ban Luo, Gang Yuan. Software: Linhan Zhai, Ping Liu. Supervision: Qiuxia Wang, Ban Luo, Gang Yuan, Jing Zhang. Validation: Jing Zhang. Visualization: Linhan Zhai, Jing Zhang. Writing—original draft: Linhan Zhai. Writing—review & editing: Jing Zhang.

ORCID iDs

Linhan Zhai
   https://orcid.org/0000-0002-1821-7852
Qiuxia Wang
   https://orcid.org/0000-0001-6536-2131
Ping Liu
   https://orcid.org/0000-0001-7161-8316
Ban Luo
   https://orcid.org/0000-0002-1257-2423
Gang Yuan
   https://orcid.org/0000-0002-0605-1568
Jing Zhang
   https://orcid.org/0000-0002-0294-4502

REFERENCES

1. Bahn RS. Graves' ophthalmopathy. *N Engl J Med* 2010;362:726-738
2. Bartalena L, Baldeschi L, Boboridis K, Eckstein A, Kahaly GJ, Marcocci C, et al. The 2016 European Thyroid Association/European Group on Graves' orbitopathy guidelines for the management of Graves' orbitopathy. *Eur Thyroid J* 2016;5:9-26
3. Vannucchi G, Covelli D, Campi I, Origo D, Currò N, Cirello V, et al. The therapeutic outcome to intravenous steroid therapy for active Graves' orbitopathy is influenced by the time of response but not polymorphisms of the glucocorticoid receptor. *Eur J Endocrinol* 2014;170:55-61
4. Sussman MS, Vidarsson L, Pauly JM, Cheng HL. A technique for rapid single-echo spin-echo T2 mapping. *Magn Reson Med* 2010;64:536-545
5. Keene KR, Beenakker JM, Hooijmans MT, Naarding KJ, Niks EH, Otto LAM, et al. T2 relaxation-time mapping in healthy and diseased skeletal muscle using extended phase graph algorithms. *Magn Reson Med* 2020;84:2656-2670
6. Chen W, Hu H, Chen HH, Su GY, Yang T, Xu XQ, et al. Utility of T2 mapping in the staging of thyroid-associated ophthalmopathy: efficiency of region of interest selection methods. *Acta Radiol* 2020;61:1512-1519

7. Das T, Roos JCP, Patterson AJ, Graves MJ, Murthy R. T2-relaxation mapping and fat fraction assessment to objectively quantify clinical activity in thyroid eye disease: an initial feasibility study. *Eye (Lond)* 2019;33:235-243

8. Hu H, Xu XQ, Chen L, Chen W, Wu Q, Chen HH, et al. Predicting the response to glucocorticoid therapy in thyroid-associated ophthalmopathy: mobilizing structural MRI-based quantitative measurements of orbital tissues. *Endocrine* 2020;70:372-379

9. Shafi F, Mathewson P, Mehta P, Ahluwalia HS. The enlarged extraocular muscle: to relax, reflect or refer? *Eye (Lond)* 2017;31:537-544

10. Gould DJ, Roth FS, Soparkar CN. The diagnosis and treatment of thyroid-associated ophthalmopathy. *Aesthetic Plast Surg* 2011;36:638-648

11. Zhang C, Lin Y, Han Z, Gao L, Guo R, Shi Q, et al. Feasibility of T2 mapping and magnetic transfer ratio for diagnosis of intervertebral disc degeneration at the cervicothoracic junction: a pilot study. *Biomed Res Int* 2019;2019:6396073

12. Del Grande F, Santini F, Herzka DA, Aro MR, Dean CW, Gold GE, et al. Fat-suppression techniques for 3-T MR imaging of the musculoskeletal system. *Radiographics* 2014;34:217-233

13. Lubner MG, Smith AD, Sandrasegaran K, Sahani DV, Pickhardt PJ. CT texture analysis: definitions, applications, biologic correlates, and challenges. *Radiographics* 2017;37:1483-1503

14. Hou K, Ai T, Hu WK, Luo B, Wu YP, Liu R. Three dimensional orbital magnetic resonance T2-mapping in the evaluation of patients with Graves' ophthalmopathy. *J Huazhong Univ Sci Technolog Med Sci* 2017;37:938-942

15. Mourits MP, Prummel MF, Wiersinga WM, Koornneef L. Clinical activity score as a guide in the management of patients with Graves' ophthalmopathy. *Clin Endocrinol (Oxf)* 1997;47:9-14

16. Bartalena L, Baldeschi L, Dickinson A, Eckstein A, Kendall-Taylor P, Marcocci C, et al. Consensus statement of the European Group on Graves' orbitopathy (EUGOGO) on management of GO. *Eur J Endocrinol* 2008;158:273-285

17. Xu L, Li L, Xie C, Guan M, Xue Y. Thickness of extraocular muscle and orbital fat in MRI predicts response to glucocorticoid therapy in Graves' ophthalmopathy. *Int J Endocrinol* 2017;2017:3196059

18. Shen L, Huang F, Ye L, Zhu W, Zhang X, Wang S, et al. Circulating microRNA predicts insensitivity to glucocorticoid therapy in Graves' ophthalmopathy. *Endocrine* 2015;49:445-456

19. Prabhakar BS, Bahn RS, Smith TJ. Current perspective on the pathogenesis of Graves' disease and ophthalmopathy. *Endocr Rev* 2003;24:802-835

20. Smith TJ, Koumas L, Gagnon A, Bell A, Sempowski GD, Phipps RP, et al. Orbital fibroblast heterogeneity may determine the clinical presentation of thyroid-associated ophthalmopathy. *J Clin Endocrinol Metab* 2002;87:385-392

21. Ohnishi T, Noguchi S, Murakami N, Tajiri J, Harao M, Kawamoto H, et al. Extraocular muscles in Graves ophthalmopathy: usefulness of T2 relaxation time measurements. *Radiology* 1994;190:857-862

22. Gold GE, Han E, Stainsby J, Wright G, Brittain J, Beaulieu C. Musculoskeletal MRI at 3.0 T: relaxation times and image contrast. *AJR Am J Roentgenol* 2004;183:343-351

23. Schlaeger S, Weidlich D, Klupp E, Montagnese F, Deschauer M, Schoser B, et al. Water T2 mapping in fatty infiltrated thigh muscles of patients with neuromuscular diseases using a T2-prepared 3D turbo spin echo with SPAIR. *J Magn Reson Imaging* 2020;51:1727-1736

24. Bednarczuk T, Gopinath B, Ploski R, Wall JR. Susceptibility genes in Graves' ophthalmopathy: searching for a needle in a haystack? *Clin Endocrinol (Oxf)* 2007;67:3-19

25. Łacheta D, Miśkiewicz P, Głuszko A, Nowicka G, Struga M, Kantor I, et al. Immunological aspects of Graves' ophthalmopathy. *Biomed Res Int* 2019;2019:7453260

26. Wang Y, Zhang S, Zhang Y, Liu X, Gu H, Zhong S, et al. A single-center retrospective study of factors related to the effects of intravenous glucocorticoid therapy in moderate-to-severe and active thyroid-associated ophthalmopathy. *BMC Endocr Disord* 2018;18:13

27. Şahlı E, Gündüz K. Thyroid-associated Ophthalmopathy. *Turk J Ophthalmol* 2017;47:94-105

28. Xing L, Ye L, Zhu W, Shen L, Huang F, Jiao Q, et al. Smoking was associated with poor response to intravenous steroids therapy in Graves' ophthalmopathy. *Br J Ophthalmol* 2015;99:1686-1691

29. Wiersinga WM. Advances in treatment of active, moderate-to-severe Graves' ophthalmopathy. *Lancet Diabetes Endocrinol* 2017;5:134-142

30. Liu P, Luo B, Chen L, Wang QX, Yuan G, Jiang GH, et al. Baseline volumetric T2 relaxation time histogram analysis: can it be used to predict the response to intravenous methylprednisolone therapy in patients with thyroid-associated ophthalmopathy? *Front Endocrinol (Lausanne)* 2021;12:614536

31. Hu H, Chen HH, Chen W, Wu Q, Chen L, Zhu H, et al. T2 mapping histogram at extraocular muscles for predicting the response to glucocorticoid therapy in patients with thyroid-associated ophthalmopathy. *Clin Radiol* 2021;76:159.e1-159.e8